A COMPREHENSIVE CONSTITUTIVE EQUATION FOR GRANULAR MATERIALS

GERD GUDEHUS

Institute for Soil Mechanics and Rock Mechanics,
University of Karlsruhe,
Engler-Bunte-Ring, D-76128 Karlsruhe, Germany
gudehus@ibf-tiger.bau-verm.uni-karlsruhe.de

(Received 16 March 2000)

Abstract: A constitutive equation is proposed for describing changes of states of granular materials, which are sufficiently characterised by the void ratio and the stress tensor. It may be considered as an extension of the Critical State concept. It is based on recently published hypoplastic equations and covers a wide range of densities, pressures and deformations. A factorial decomposition allows a rather easy separation and determination of material parameters. Two factors depend on a relative void ratio so that it remains within lower and upper bounds. The bounding void ratios decrease monotonously from maximal values to zero with increasing pressure. The same reduction of the void ratio is proposed for an isotropic compression starting from a suspension. Thus a granulate hardness is defined, and a stiffness factor can be determined. Four material parameters can be estimated from classification tests and determined from the asymptotic behaviour in element tests. Four further parameters are determined by calibration; they are rather constant for wide groups of materials. Strength and stiffness values can be derived and used for the analysis of deformations, stability, and flow. The viscous behaviour is modelled by a rate dependent factor with one further parameter. Limitations and possible extensions of this comprehensive approach are also outlined.

Keywords: constitutive equation of soil, critical state, deformation, granular material, stability analysis

1. Position and objectives

The aim of this paper is to describe mathematically certain mechanical changes of state of granular materials. The grains may be mineral or of other nature, convex and of arbitrary sizes. The grain material may be ideally elasto-visco-plastic and incompressible. A pore fluid may be present, but no cementation. The following simplifying assumptions are made.

The state of the solid constituent is assumed to be fully described by the void ratio e, the Cauchy granulate stress tensor $\boldsymbol{T}_s$ and the velocity $\boldsymbol{v}_s$ of the grain skeleton.

This assumption excludes higher order pores, clods and more complicated stress tensors (Section 4.2). $\boldsymbol{T}_s$ may also be called the inter-granular or effective stress tensor. We use the sign convention of general mechanics and the subscripts of the theory of mixtures (*e.g.* De Boer and Ehlers 1990). The pressure p_f of the pore fluid is assumed to yield the total stress tensor by:

$$\boldsymbol{T} = \boldsymbol{T}_s - p_f \mathbf{1}, \tag{1}$$

with the unit tensor **1**. Degrees of saturation other than 0 or 1 are excluded for brevity's sake.

A constitutive equation determines the objective rate of granulate stress, defined by:

$$\mathring{\boldsymbol{T}}_s := \dot{\boldsymbol{T}}_s + \boldsymbol{W}_s \boldsymbol{T}_s - \boldsymbol{T}_s \boldsymbol{W}_s, \tag{2}$$

as a function of the granulate stretching rate $\boldsymbol{D}_s := (\nabla \boldsymbol{v}_s + \boldsymbol{v}_s \nabla)/2$, *i.e.* the symmetric part of the gradient $\nabla \boldsymbol{v}_s$ (antimetric part $\boldsymbol{W}_s := (\nabla \boldsymbol{v}_s - \boldsymbol{v}_s \nabla)/2$). e and $\boldsymbol{T}_s$ enter this function. With the assumed incompressibility of the grains, the rate of change of the void ratio is (*e.g.* Gudehus 1981):

$$\dot{e} = (1 + e)\, \mathrm{tr}\, \boldsymbol{D}_s . \tag{3}$$

We exclude changes of state which cannot be achieved by homogeneous deformations, such as the destruction or production of higher order pores or clods (Section 4.2). Our constitutive equation therefore has the general shape:

$$\mathring{\boldsymbol{T}}_s = \boldsymbol{F}(e, \boldsymbol{T}_s, \boldsymbol{D}_s) \tag{4}$$

with a tensor-valued function $\boldsymbol{F}$ of e, $\boldsymbol{T}_s$ and $\boldsymbol{D}_s$.

$\boldsymbol{F}$ has a certain mathematical representation so that all granular materials thus defined are assumed to be equal in quality. Using notions with Greek names proposed by Kolymbas (1991), the following properties have to be covered, *viz.*:

— hypoplasticity (analogous to hypoelastic indicating the lack of yield surface and flow rule): $\boldsymbol{F}$ is a non-linear function of $\boldsymbol{D}_s$ and approximately positively homogeneous of first order, *i.e.* $\boldsymbol{F}(\boldsymbol{D}_s) \neq -\boldsymbol{F}(-\boldsymbol{D}_s)$ and $\boldsymbol{F}(\lambda \boldsymbol{D}_s) \approx \lambda \boldsymbol{F}(\boldsymbol{D}_s)$, $\lambda > 0$;

— pyknotropy (greek for density-dependent): $\boldsymbol{F}$ depends explicitly on density, *i.e.* void ratio e;

— barotropy (greek for pressure-dependent): the norm of $\boldsymbol{F}$ increases with $-\mathrm{tr}\boldsymbol{T}_s$ (*i.e.* mean pressure) weaker than linearly, *i.e.* $\| \boldsymbol{F}(\lambda \boldsymbol{T}_s) \| < \lambda \| \boldsymbol{F}(\boldsymbol{T}_s) \|$, $\lambda > 0$;

— argotropy (greek for velocity-dependent): the norm of $\boldsymbol{F}$ increases, though weakly, with the stretching rate, *i.e.* $\| \boldsymbol{F}(\lambda \boldsymbol{D}_s) \| > \lambda \| \boldsymbol{F}(\boldsymbol{D}_s) \|$, if $\lambda >> 1$.

Pyknotropy and barotropy are unified as they are physically non-separable. Recent versions of hypoplastic constitutive relations (*e.g.* Bauer and Wu 1993) have these properties. Representations of $\boldsymbol{F}$ should satisfy, however, more requirements, *viz.*:

— unit invariance: $\boldsymbol{F}$ is not changed by a change of units;

— closedness: an allowable subspace of states cannot be left by arbitrary deformation histories with constant mean pressure;

— separability: material parameters defined by $\boldsymbol{F}$ can be determined separately.

Unit invariance can be satisfied by using suitable material parameters of the grains. Barotropy requires at least one parameter with the unit of stress (Section 2.4). Argotropy calls for a reference time which is practically constant for different granular materials (Section 2.5).

The notion of closedness is linked with the one of limit states. Deformations with constant mean stress cannot lead out of a certain region of the ($\boldsymbol{T}_s$, e)-space. Earlier versions of hypoplastic relations can lead to unacceptable stress states which are excluded in more recent versions (*e.g.* Kolymbas and Wu 1993). The requirement is extended here to void ratios.

Separability is a pragmatic requirement: the more it is satisfied, the easier can the material parameters be determined (Section 3.1). This gain of feasibility may be at the cost of fitting quality. The constitutive equation thus becomes also more transparent and robust.

This paper is an attempt to close the present gap between geotechnical experts and specialists for constitutive relations. Recent versions of hypoplastic relations (*e.g.* Wu and Bauer 1993) already cover a wide range of deformations, void ratios and pressures. The present constitutive equation is more comprehensive, simpler and physically more appealing. The proposed concept allows us to leave aside initial states (which are often poorly defined), to separate more clearly qualitative and quantitative properties and to determine the latter with simple procedures. Various familiar notions are avoided: stiffness and strength are not material parameters, but derived for special states and directions of stretching rate, and there is no elastic range in a stress or strain space. On the other hand, some properties well known from conventional soil mechanics are incorporated.

This approach may be looked upon as an extension and modification of the Critical State concept (Schoefield and Wroth 1968):

— granulate stress ratios become constant independently of mean pressure for unlimited deformations with constant direction and volume;

— the void ratios for such states and for isotropic compression decrease in the same manner with increasing mean pressure;

— the envelope of peak stress states starts from zero and is curved, so that an effective cohesion appears only as an intercept when the envelope is linearized.

Hypoplasticity is used instead of elastoplasticity for the extension of this concept to other stress and stretching rate ratios. The compression law is modified so that a wider pressure range is covered. The word critical is retained for convenience although it is not justified in a physical sense.

One main aim is to describe the mechanical behaviour with a minimum number of parameters (Section 3.1). They can be determined from reconstituted samples, *i.e.* they represent properties which are not lost by arbitrary deformations. Further parameters are considered as rather constant for a wide class of materials. The price for this simplicity are some limitations (Section 4.1). This paper deals with qualitative aspects. More quantitative aspects of calibration are dealt with in a paper by Bauer (1996).

The general constitutive equation is introduced in Section 2.1. The implied functions and parameters are explained in Sections 2.2 to 2.5 by considering triaxial and biaxial deformations and then simple shearing. The theory is further explained in Section 3 by showing how to analyse deformations, stability and flow. Some possible extensions are indicated in Section 4.2.

2. Equation and explanation

2.1 General

The proposed constitutive equation can be written as:

$$\overset{\circ}{\boldsymbol{T}}_s = f_b f_e \left[\boldsymbol{L}\left(\hat{\boldsymbol{T}}_s, \boldsymbol{D}_s\right) + f_d \boldsymbol{N}\left(\hat{\boldsymbol{T}}_s\right) \| \boldsymbol{D}_s \| \right]. \tag{5}$$

$\hat{\boldsymbol{T}}_s := \boldsymbol{T}_s / \mathrm{tr}\, \boldsymbol{T}_s$, denotes the so-called granulate stress ratio tensor; it has the same directions of principal axes as $\boldsymbol{T}_s$. $\| \boldsymbol{D}_s \| := \sqrt{\mathrm{tr}\, \boldsymbol{D}_s^2}$ is the Euclidean norm of $\boldsymbol{D}_s$. The factors stand for barotropy (f_b) and pyknotropy (f_e and f_d). f_e and f_d depend on relative void ratios (Section 2.3). f_b is proportional to a granulate hardness and depends also on e (Section 2.4). A rate-dependent correction (Section 2.5) leaves the other properties of Equation (5) unchanged.

The tensor-valued function $\boldsymbol{L}$ is linear with respect to $\boldsymbol{D}_s$. The term with $\| \boldsymbol{D}_s \|$ is non-linear, but also homogeneous of first order with respect to $\boldsymbol{D}_s$ as required by hypoplasticity. It implies a switch function instead of the one(s) in elastoplasticity.

$\boldsymbol{L}$ and $\boldsymbol{N}$ can be represented (Bauer 1996) by:

$$\boldsymbol{L} := a_1^2 \boldsymbol{D}_s + \hat{\boldsymbol{T}}_s \,\mathrm{tr}\left(\hat{\boldsymbol{T}}_s \boldsymbol{D}_s\right), \tag{6}$$

$$\boldsymbol{N} := a_1\left(\hat{\boldsymbol{T}}_s + \hat{\boldsymbol{T}}_s^*\right), \tag{7}$$

where $\hat{\boldsymbol{T}}_s^* := \hat{\boldsymbol{T}}_s - (1/3)\boldsymbol{1}$ denotes the deviator of $\hat{\boldsymbol{T}}_s$. The factor a_1 depends on $\hat{\boldsymbol{T}}_s^*$ via:

$$\frac{1}{a_1} := c_1 + c_2 \| \hat{\boldsymbol{T}}_s^* \| \left[1 + \cos(3\theta) \right], \tag{8}$$

with the modulus $\| \hat{\boldsymbol{T}}_s^* \| := \sqrt{\mathrm{tr}\, \hat{\boldsymbol{T}}_s^{*2}}$ and the Lode parameter $\cos(3\theta) = -\sqrt{6}\, \mathrm{tr}(\hat{\boldsymbol{T}}_s^{*3}) / [\mathrm{tr}(\hat{\boldsymbol{T}}_s^{*2})]^{3/2}$. The constants c_1 and c_2 are determined by a friction angle as outlined in Section 2.2.

$\boldsymbol{L}$ is positive definite with respect to $\boldsymbol{D}_s$ so that the response envelope (Gudehus 1979) is elliptic (Bauer 1996). Its origin is shifted by $f_b f_e f_d \boldsymbol{N} \| \boldsymbol{D}_s \|$ so that it cannot leave the elliptic range (Wu and Bauer 1993). Equation (5) is not generally invertible to $\boldsymbol{D}_s$ as a function of $\overset{\circ}{\boldsymbol{T}}_s$. One should avoid calling $\overset{\circ}{\boldsymbol{T}}_s$ the cause of $\boldsymbol{D}_s$ or vice versa therefore.

So-called critical states (e_s, T_{sc}), defined by $\overset{\circ}{\boldsymbol{T}}_s = \boldsymbol{0}$ and $\dot{e} = 0$ with $f_d = 1$ (Section 2.2) are represented by a cone in the space of stress components. This cone is smooth and lies within the range of negative normal components. The cone and the associated stretching rate directions, which are generally defined by $\vec{\boldsymbol{D}}_s := \boldsymbol{D}_s / \|\boldsymbol{D}_s\|$, are obtained (Bauer 1996) from:

$$\operatorname{tr} \vec{\boldsymbol{D}}_{sc} = 0; \quad \vec{\boldsymbol{D}}_{sc} = -\mathcal{L}^{-1}\left(\hat{\boldsymbol{T}}_{sc}\right) \boldsymbol{N}\left(\hat{\boldsymbol{T}}_{sc}\right), \tag{9}$$

wherein the fourth order tensor $\mathcal{L}$ is defined by:

$$\boldsymbol{L}\left(\hat{\boldsymbol{T}}, \boldsymbol{D}_s\right) = \mathcal{L}\left(\hat{\boldsymbol{T}}\right) \boldsymbol{D}_s .$$

The two factors f_e and f_d keep e within prescribed limits for a given mean granulate pressure $p_s := -\operatorname{tr} \boldsymbol{T}_s / 3$ (Section 2.3). The dependence of these limits on p_s will enable us to calculate the factor f_b in Section 2.4.

A dilatancy ratio is defined by:

$$\kappa := \frac{\operatorname{tr} \boldsymbol{D}_s}{\| \boldsymbol{D}_s \|} \quad \text{for} \quad \operatorname{tr} \overset{\circ}{\boldsymbol{T}}_s = 0. \tag{10}$$

It can be calculated from Equation (5) as:

$$\kappa := -f_d \operatorname{tr} \boldsymbol{N}\left(\hat{\boldsymbol{T}}_s\right) \frac{\operatorname{tr} \vec{\boldsymbol{D}}_s}{\operatorname{tr} \boldsymbol{L}\left(\hat{\boldsymbol{T}}_s, \vec{\boldsymbol{D}}_s\right)} \tag{11}$$

and is needed for analyzing pyknotropy (Section 2.3) and stability (Section 3.2). An iterative procedure is required in general as $\vec{\boldsymbol{D}}_s$ is not known in advance. If κ is negative, $-\kappa$ is also called contractancy ratio. Proportional compressions (subscript p) are defined for constant directions $\vec{\boldsymbol{D}}_s = \vec{\boldsymbol{D}}_{sp}$ with $\operatorname{tr} \vec{\boldsymbol{D}}_{sp} < 0$ by:

$$\hat{\boldsymbol{T}}_{sp} = \hat{\overset{\circ}{\boldsymbol{T}}}_{sp} . \tag{12}$$

With Equation (5) this equation leads to:

$$\hat{\boldsymbol{T}}_{sp} \operatorname{tr}\left[\boldsymbol{L}\left(\hat{\boldsymbol{T}}_{sp}, \hat{\boldsymbol{D}}_{sp}\right) + f_d \boldsymbol{N}\left(\hat{\boldsymbol{T}}_{sp}\right)\right] = \boldsymbol{L}\left(\hat{\boldsymbol{T}}_{sp}, \hat{\boldsymbol{D}}_{sp}\right) + f_d \boldsymbol{N}\left(\hat{\boldsymbol{T}}_{sp}\right). \tag{13}$$

Special cases occur in the analysis of barotropy (Section 2.4) and consolidation (Section 3.2).

2.2 Critical states

We first consider stretching rates $\boldsymbol{D}_s$ so that $\dot{e} = 0$ (*i.e.* $\operatorname{tr} \boldsymbol{D}_s = 0$ from Equation (3)) and $\overset{\circ}{\boldsymbol{T}}_s = \boldsymbol{0}$. e then is called critical void ratio e_c. More precisely, $e = e_c$ is assumed to remain constant for a certain mean granulate pressure p_s, a certain

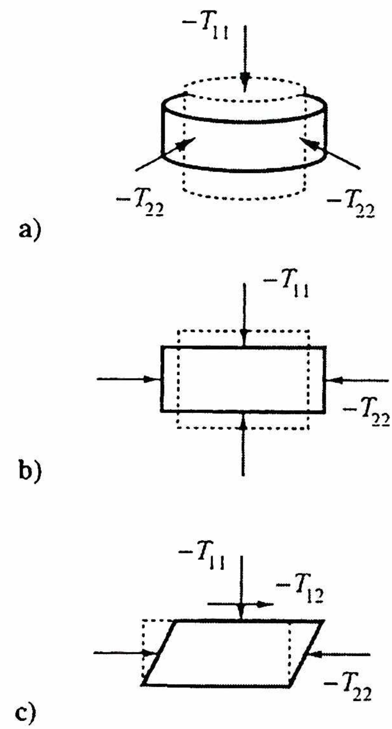

Figure 1. *Cases enabling critical states*

stretching rate direction $\vec{D}_{sc}$, and a stress ratio tensor $\hat{T}_{sc}$ associated with this $\vec{D}_{sc}$ by Equation (9). We can neglect argotropy (Section 2.5). The subscript *s* is dropped in the sequel as long as the influence of a pore fluid is not considered.

We now analyze some special cases. A cylindrical compression (Figure 1a), defined by $-T_{11} > -T_{22} = -T_{33}$ (conventionally $\sigma_1 > \sigma_2 = \sigma_3$) is carried out with constant mean stress (*i.e.* $\mathrm{tr}\,\dot{\boldsymbol{T}} = \dot{T}_{11} + 2\dot{T}_{22} = 0$) up to a plateau $\dot{T}_{11} = 0$. $\dot{e} = 0$ implies zero dilatancy, *i.e.* $D_{11} + 2D_{22} = 0$ (conventionally $\dot{\varepsilon}_1 + 2\dot{\varepsilon}_2 = 0$). The stress ratio is then defining a critical friction angle φ_c by:

$$\sin^2\varphi_c := \left(\frac{T_{11} - T_{22}}{T_{11} + T_{22}}\right)_c^2 . \tag{14}$$

Equations (5) to (8) yield, with $f_d = 1$, $D_{11} = -1$ and $D_{22} = D_{33} = 1/2$ (zero mixed components), two homogeneous equations for the critical stress ratio, *viz.* $\dot{T}_{11} = \dot{T}_{22} = 0$. With a cylindrical extension defined by $-T_{11} < -T_{22} = -T_{33}$, one can also reach a critical state for a given mean pressure, *i.e.* $\dot{T}_{11} = \dot{T}_{22} = 0$ with $f_d = 1$, $D_{11} = 1$ and $D_{22} = D_{33} = -1/2$. Equation (14) is postulated to hold with the same pressure-independent φ_c as for cylindrical compression. One can thus calculate the two constants in Equation (8), namely:

$$c_1 = \sqrt{\frac{3}{8}}\frac{(3-\sin\varphi_c)}{\sin\varphi_c}, \qquad c_2 = \frac{3}{8}\frac{(3+\sin\varphi_c)}{\sin\varphi_c} \tag{15}$$

as outlined by Bauer (1996).

We now turn to biaxial deformations, *i.e.* $D_{33} = 0$ and zero mixed components (Figure 1b). Critical states with constant mean pressure imply $D_{11} = -D_{22}$ and Equation (14) again. Using Equations (5) – (8) with $f_d = 1$, one has $\dot{T}_{11} = 0$ and $\dot{T}_{22} = 0$. Defining φ_c by Equation (14) for cylindrical compression, one thus obtains a slightly higher critical friction angle.

Similar results can be obtained for cuboidal deformations leading to critical states, *i.e.* $D_{22} \neq D_{33}$ and $D_{11} = -D_{22} - D_{33}$. Simple shearing (Figure 1c) can be treated in the same manner. Using Equations (5) – (8) as before one obtains a slightly higher $\varphi_c = \arctan(-T_{12}/T_{11})_c$ than for cylindrical compression.

We stipulate φ_c as the friction angle for a critical state under triaxial compression. Angles for other critical states can be calculated using Equations (5) and (9). They will, however, scarcely be needed, as not even stationary flow generally implies $\dot{e} = 0$ and $\mathring{\boldsymbol{T}}_s = \boldsymbol{0}$ (Section 3.4).

2.3 Pyknotropy and dilatancy

We now leave states with $e = e_c$, but still without considering barotropy (by assuming constant granulate pressure p_s) and argotropy. We introduce a void ratio of maximum densification, e_d, by postulating $f_d = 0$ in Equation (5) for $e = e_d$ (the dependence of e_d on p_s will be outlined in Section 2.4). The constitutive equation becomes hypoelastic for $f_d = 0$, *i.e.* linear with respect to $\boldsymbol{D}_s$. For $e > e_d$, f_d is required to increase monotonously up to $f_d = 1$ with the relative void ratio:

$$r_e := \frac{e - e_d}{e_c - e_d}. \tag{16}$$

$1 - r_e$ comes rather close to the usual density index I_d for sandy soils and to the consistency index I_c for clayey soils (Section 3.1). A suitable representation of f_d is:

$$f_d = r_e^{\alpha} \qquad (r_e \geq 0) \tag{17}$$

with a parameter α which is rather constant ($0.1 < \alpha < 0.3$) for a wide class of materials (Bauer 1996).

We now consider peaks (subscript P) under cylindrical compression with constant mean stress, *i.e.* $\dot{T}_{11} = 0$ and $\dot{T}_{22} = 0$ with $e_d \leq e < e_c$. A peak friction angle φ_P *is* defined by:

$$\sin^2\varphi_P := \left(\frac{T_{11} - T_{22}}{T_{11} + T_{22}}\right)_P^2 \tag{18}$$

and can be calculated from Equation (5) with $\dot{T}_{11} = 0$. The corresponding peak dilatancy ratio can be calculated from Equation (11) as:

$$\kappa_P = \left[(D_{11} + 2D_{22}) / \sqrt{D_{11}^2 + 2D_{22}^2} \right]_P .$$

Both φ_p and κ_p decrease with increasing relative void ratio r_e. f_d controls the relative height of a peak (Bauer 1996).

Other peak friction angles and dilatancy ratios are obtained for cylindrical extension and biaxial deformation. For simple shearing, a peak friction angle $\varphi_p = \arctan(-T_{12}/T_{22})_p$ and a peak dilatancy angle $v_p := \arctan(D_{11}/D_{12})_p$ can be calculated. An extension to other deformations, *i.e.* stretching with any direction, is possible. Such peak values can be helpful for the analysis of stability (Section 3.2).

The other pyknotropy factor f_e in Equation (5) is to determine the influence of the void ratio on the position of the peak under constant mean pressure. f_e is mainly influenced by the ratio e_c/e. A simple adequate representation for f_e is (Bauer 1996):

$$f_e := \left(\frac{e_c}{e} \right)^\beta , \tag{19}$$

with a rather constant exponent in the narrow range $1 < \beta < 1.1$.

The effect of f_e can be illustrated for a cylindrical compression (Figure 2). The height h may be reduced with increasing axial pressure $-T_{11}$ and $T_{11} + 2T_{22} =$ const (a). One can calculate the change of void ratio (b) and stress ratio (c) by means of Equation (5) with Equations (3), (17), (19), $D_{11} = \dot{h}/h$, and the factor a_1 from Equations (8) and (15).

With $e = e_d$ initially, the dilatancy ratio (κ from Equation (10), and then $-D_{22}/D_{11}$ from κ) increases from zero to a maximum and decreases beyond it to zero when e approaches e_c (Figure 2b). With $e = e_c$ initially, κ increases from a negative value, reaches a small positive amount with a slight reduction of e, and tends to zero with $e \to e_c$. The peak is highest and lefternmost for $e = e_d$ initially, and the opposite is true for $e = e_c$ initially. Intermediate curves are obtained for $e_d < e < e_c$ initially. f_e thus controls the position of a peak.

Similar curves can be calculated for cylindrical extension, biaxial deformation and simple shearing. Void and stress ratios cannot leave a range given by e_c, e_d and φ_P for a constant mean pressure. (Ratios outside are possible with substantial changes of mean pressure, Section 2.4).

The meaning of e_d can be illustrated for repeatedly reversed cylindrical deformations under constant mean pressure (Figure 3, system as in Figure 1a). The height is changed cyclically, and the lateral pressure is adapted so that $T_{11} + 2T_{22} =$ const. The changes of void ratio (a) and stress ratio (b) can be calculated with Equations (3), (5), (17), (19). Starting with $e = e_c$, the first curve sections of e and T_{11}/T_{22} versus $(h - h_0)/h_0$ can be as in Figures 1b and 1c. The sections after each reversal are calculated correspondingly. If the stretching $(h - h_0)/h_0$ is small enough, there is an excess of contractancy so that e is reduced. The lower bound e_d is approached with a low amplitude and a large number of cycles. With higher stretching amplitudes e can again be increased up to the upper bound e_c. Similar calculations can be made for biaxial deformation and simple shearing (Bauer 1996).

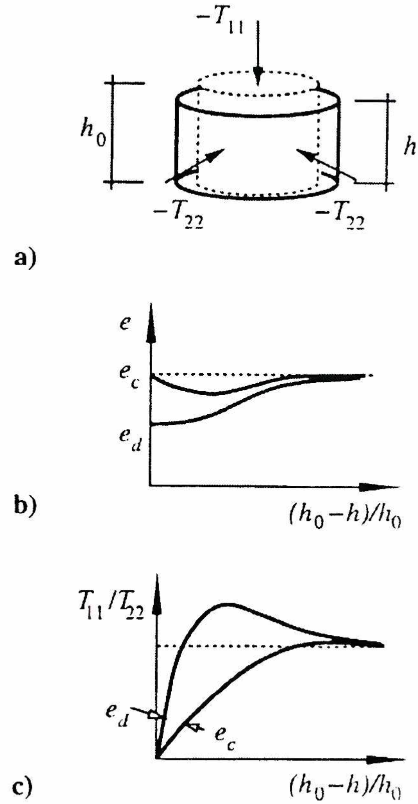

***Figure 2*.** *Cylindrical compression with constant mean pressure*

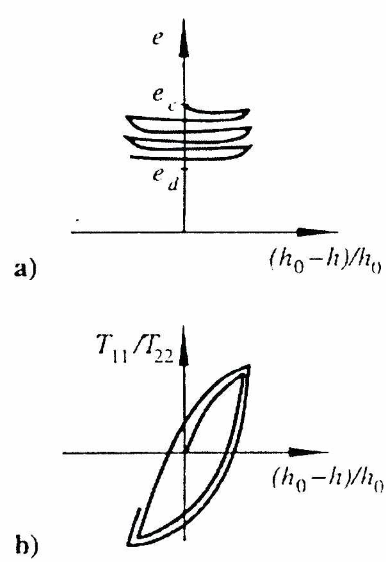

Figure 3. *Effect of cyclic changes of height of a cylinder under constant mean pressure*

2.4 Barotropy

In order to determine the pressure dependence of the factors in Equation (5) we now consider proportional compressions as defined in Section 3.1. We begin with an isotropic proportional compression (subscript i) defined by $\boldsymbol{D}_s = -\mathbf{1}$ and $\boldsymbol{T}_s = -p_s\mathbf{1}$, starting from a suspension. It is proposed (Bauer 1996) that the void ratio, e_i then, decreases with the mean pressure p_s according to:

$$e_i = e_{i0} \exp\left[-\left(\frac{3p_s}{h_s}\right)^n\right], \tag{20}$$

with a constant exponent $0.3 < n < 0.5$. The granulate hardness h_s defined by Equation (20) represents the compliance of the grain skeleton depending on the pressure level. The skeleton originates with $e = e_{i0}$ for $p_s = 0$.

It is postulated that the limiting void ratios e_c and e_d decrease with the mean pressure as e_i, *i.e.*:

$$e_c = e_{c0} \exp\left[-\left(\frac{3p_s}{h_s}\right)^n\right], \tag{21}$$

$$e_d = e_{d0} \exp\left[-\left(\frac{3p_s}{h_s}\right)^n\right], \tag{22}$$

with the same constants n and h_s as in Equation (20), and two material constants e_{c0} and e_{d0}. e_{i0} is required to exceed e_{c0} slightly with a certain ratio, *i.e.*:

$$e_{i0} = \lambda\, e_{c0}, \tag{23}$$

with a material constant $1.1 < \lambda < 1.5$. Plotting void ratios versus mean pressure (Figure 4) yields three affinous curves. The ones for e_i and e_c are close to those of the original Cam Clay theory in a certain range of pressures, but they are also consistent for $0 \leftarrow p_s \rightarrow \infty$.

We now insert e_c and e_d from Equations (21), (22) into the constitutive equation, Equation (5), with Equations (17), (19). The ratios of void ratios r_e and e_c/e do not directly depend on the mean pressure. The rate of mean pressure under isotropic proportional compression, $\dot{p}_s$, can be calculated from Equations (5) – (8), (17), (19), (23) as:

$$3\dot{p}_s = \frac{\dot{e}_i}{1+e_i} f_b \lambda^{-\beta} \left(\frac{1}{c_1^2}\right) \times \left[1 + \frac{c_1^2}{3} - \left(\frac{\lambda - e_{d0}/e_{c0}}{1 - e_{d0}/e_{c0}}\right)^\alpha \frac{c_1}{\sqrt{3}}\right], \tag{24}$$

and from Equation (20) as:

$$3\dot{p}_s = \frac{\dot{e}_i}{e_i} \frac{h_s}{n} \left(\frac{3p_s}{h_s}\right)^{1-n}. \tag{25}$$

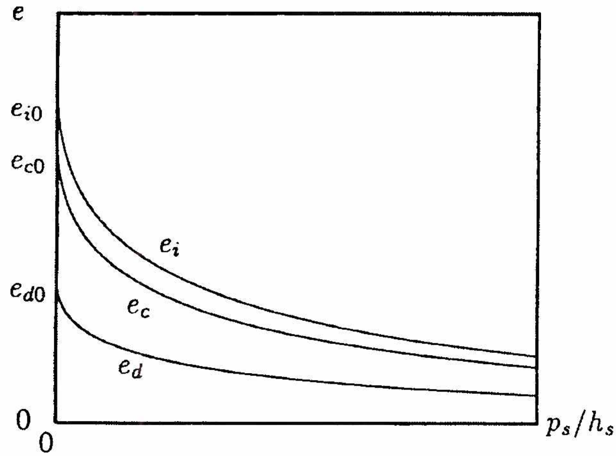

Figure 4. *Pressure dependence of void ratios*

From these two equations we obtain:

$$f_b = \frac{h_s}{n}\frac{1+e_i}{e_i}\lambda^{\beta}\left(\frac{3p_s}{h_s}\right)^{1-n}\left(\frac{1}{c_1^2}\right)\times\left[1+\frac{c_1^2}{3}-\left(\frac{\lambda-e_{i0}/e_{c0}}{1-e_{i0}/e_{c0}}\right)^{\alpha}\frac{c_1}{\sqrt{3}}\right]^{-1}, \tag{26}$$

which is postulated to generally hold in Equation (5).

The transition to other proportional compressions is straightforward. For a one-dimensional compression, *e.g.* with $D_{11}=-1$ and $D_{ij}=0$ otherwise (subscript 0) one has to calculate first the stress ratio $K_0 := T_{22} / T_{11} = T_{33} / T_{11}$ (subscript s omitted) from the condition $D_{22}=0$ with Equation (5). As far as the void ratio, called e_0 then, decreases with p_s as e_c and e_d, f_d is independent of tr $\boldsymbol{T}_s$, and therefore K_0, too. Equalizing $\dot{e}_0$ from Equation (5) and from Equation (22) with e_{00} instead of e_{c0} yields a formula like Equation (26) except for the factors which are independent of e and p_s. As f_b is required to be the same, one can thus determine e_{i0}, n and h_s as well from oedometer tests (Bauer 1996).

A similar calculation can be made for a proportional compression without shearing, *i.e.* $D_{11}=-1$, $D_{22}=-a$; $D_{33}=-b$ and zero mixed components. Two stress ratios, T_{22} / T_{11} and T_{33} / T_{11}, are obtained from Equation (5), *i.e.* two cubic equations independent of p_s. The void ratio decreases with p_s as e_i, and its value for $p_s = 0$ can be calculated. For more general proportional compressions (subscript p) the stress ratios are obtained with Equation (13) from D_{sp}, Equation (21) holds with e_{p0} instead of e_{c0} and e_{p0} can be calculated as outlined above.

With the aid of Equation (20), an equivalent pressure can be defined as:

$$p_e := \frac{1}{3}h_s\left[\ln\left(\frac{e_{i0}}{e}\right)\right]^{1/n}, \tag{27}$$

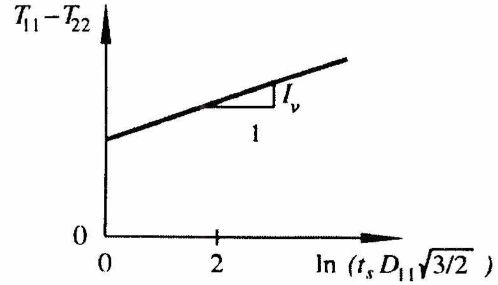

Figure 5. Drained cylindrical compression at critical states with different stretching rates

which is useful for the estimation of stiffness and strength values (Sections 3.2 and 3.3). With the factor $3/(1+2K_0)$ and e_{00} instead of e_{i0}, p_e can likewise be defined for one-dimensional compression as proposed by Hvorslev (1960).

2.5 Argotropy

The rate-dependence of granular materials, which has as yet been neglected, can be accounted for by introducing an argotropic granulate hardness:

$$h_{sa} = h_s \left(\| \mathbf{D}_s \| t_s \right)^{I_v} \tag{28}$$

instead of h_s into Equations (20) – (22). t_s is a characteristic time of the solid constituent. Leinenkugel (1976) has shown, using the theory of rate processes, that t_s can be fixed arbitrarily for a constant absolute temperature T. Leaving aside substantial changes of T, one can choose t_s so that $h_{sa} = h_s$ results for a convenient modulus of the stretching rate. We thus have only one parameter for argotropy, namely I_v (which is linked with t_s).

A consequence can be shown for a drained cylindrical compression with constant void ratio but variable rate (Figure 5). Initially, $\sqrt{3/2}D_{11}$ (= $\|\mathbf{D}_s\|$ in this case) may be equal to $1/t_s$ so that $h_{sa} = h_s$ results from Equation (28). An increase of D_{11} leads to an increase of $(T_{22} - T_{11})$ which is approximately proportional to $I_v \ln (t_s D_{11})$. This relationship was introduced by Leinenkugel (1976), calling I_v viscosity index. It was repeatedly confirmed and can be widely used (*e.g.* Gudehus 1984). For soils I_v lies between about 0.01 (quartz sand) and 0.05 (fat clay). A change of the magnitude of the stretching rate is therefore only of importance if it reaches several orders of magnitude. Argotropy is also of importance for uncommonly low or high gradients of velocity (Section 3.2). Our simple approach cannot, however, cover the whole spectrum of argotropy (Section 4.1).

3. Applications

3.1 Determination of parameters

We end up with only five material parameters, *viz.*:

h_s — granulate hardness for $\|\mathbf{D}_s\| = 1/t_s$;

φ_c — critical friction angle;

e_{c0} — critical void ratio for zero inter-granular stress;
e_{d0} — void ratio of maximum densification for zero inter-granular stress;
I_v — viscosity index.

They can be estimated from classification tests a more precisely determined by modified standard tests. The additional constants α, β, n, λ are considered rather constant for a wide class of granular materials. They can be determined by element tests (Bauer 1996).

Classification tests are rather simple for hard-grained coarse granular materials. φ_c is close to the slope angle of the loose dry material. e_{c0} is close to the usual void ratio of the fully dilated material, and e_{d0} is obtained by shaking, so that $1 - r_e$ from Equation (17) comes close to the usual density index I_d. h_s is proportional to the strength of the grain material.

Fine granular materials can have higher order pores for very low pressures so that the proposed theory becomes invalid (Section 4.2). This can be avoided by exceeding a h_s-dependent minimum inter-granular pressure. In order to avoid capillary effects and to allow for the influence of the band pore fluid, one should test the saturated material. h_s can be estimated from a shrinkage test with controlled relative humidity ψ of the air. As long as the sample is not drying out, the granulate pressure at a thermodynamic equilibrium with $T \approx 290$ kPa amounts to $1.35 \cdot 10^5$ kPa $\cdot \ln(1/\psi)$ according to Kelvin's formula. From the equilibrium water contents w_1, and w_2 for the humidities $\psi_1 \approx 1$ and $\psi_2 < 1$ one can, with Equation (20), then calculate:

$$h_s \approx 3 \cdot 1.35 \cdot 10^5 \text{kPa} \cdot \frac{\ln\left(\frac{1}{\psi_2}\right)}{\left[\ln\left(\frac{w_1}{w_2}\right)\right]^{1/n}}, \tag{29}$$

wherein $e = w\gamma_s/\gamma_f$ (with the specific weights γ_s and γ_f of solid and fluid) is used. A crude estimate is obtained with $w_1 = w_L$ (liquid limit) and $w_2 = w_s$ (shrinkage limit).

φ_c can be rather easily estimated from a drained simple shear test with a thin layer of saturated material between two filter plates without end restraint, and with $\psi = 1$ or under water to avoid shrinking.

e_{c0} can be estimated from the liquid limit w_L using Equation (21) as:

$$e_{c0} \approx w_L \frac{\gamma_s}{\gamma_f} \exp\left[-\left(\frac{3p_L}{h_s}\right)^n\right]. \tag{30}$$

The order of magnitude of the inter-granular pressure reached in this test is equal to the maximal pressure during each blow, *viz.* $p_L \approx 5$ kPa. e_{d0} is related to the plasticity limit w_P by:

$$e_{d0} \approx w_P \frac{\gamma_s}{\gamma_f} \exp\left[-\left(\frac{3p_P}{h_s}\right)^n\right], \tag{31}$$

wherein the inter-granular pressure during this test is approximately $p_p \approx 15$ kPa. The appearance of cracks indicates the end of contractancy under cyclic shearing as depicted by Figure 3. Thus $1 - r_e$ from Equation (17) comes rather close to the usual consistency index I_c.

Modified standard tests yield more precise parameters and supply a basis for correlations. h_s can be obtained from oedometer tests, φ_c from triaxial compression tests, and e_{c0} and e_{d0} can be found from filling with uniform granular flow and subsequent cyclic shearing. I_v is obtained from triaxial tests with jumps of stretching rate, or from secondary compression tests with an oedometer (Leinenkugel 1976).

Element tests serve to justify simpler standard tests to determine the constants α, β, n, λ by calibration, and to detect limitations of the proposed constitutive equation. By definition, they require homogeneous samples and uniform deformations, which is only possible to a certain extent. It is advisable to start with a high void ratio in order to suppress localisations, which is best achieved by filling with stationary flow. Walls of the testing chamber cause some non-uniformity of flow and packing, if the sample is not frozen and cut. It appears that triaxial tests with short samples, smooth non-rotating end platens, and repeated change of compression and extension with increasing pressure, and also special oedometer tests, are apt to avoid these shortcomings (Bauer 1996).

3.2 Deformations

The proposed constitutive equation can be used to predict deformations of granular bodies caused by changes of boundary conditions, *e.g.* by static loading, drainage or excavation. We consider first undelayed deformations and then those which are delayed by viscosity.

An initial state of a granular body is defined by a spatial distribution of material parameters (h_s, φ_c *etc.*) and state variables (e, $\boldsymbol{T}_s$) at a time t_0. The choice of t_0 is arbitrary: start or end of sedimentation or filling, ground improvement, construction works *etc*. As the mechanical past is never fully known nor analysable, one can never precisely determine an initial state. Simplified fields of parameters and state variables have to be used, which makes the prediction of subsequent deformations inevitably uncertain. This fact justifies some simplifications and calls for monitoring and compensating technical actions.

Differential stiffness values needed for numerical procedures are determined from the constitutive equation. The differential stiffness matrix, a fourth order non-symmetric tensor defined by $\overset{\circ}{\boldsymbol{T}}_s = \mathcal{M}\boldsymbol{D}_s$, is calculated from Equation (5) as:

$$\mathcal{M} = f_b f_e \left[\mathcal{L}\left(\hat{\boldsymbol{T}}_s\right) + f_d \boldsymbol{N}\left(\hat{\boldsymbol{T}}_s\right)\vec{\boldsymbol{D}}_s^{-1} \right]. \tag{32}$$

Thus $\mathcal{M}$ depends on the direction $\vec{\boldsymbol{D}}_s$ of the granular stretching rate which has to be determined by iteration. Convergence has been achieved in several cases more easily than with elastoplastic approaches. However, an extremely wide spectrum of $\mathcal{M}$ can still cause numerical problems.

The boundary conditions for deformation problems are also partly arbitrary, but at least consistency with the constitutive equation should be maintained. Free boundaries — touching gas or fluid — are rather clear. Interfaces to walls, slabs, inclusions *etc.* can be the origin of localisation (Section 4.2). It is advisable to include foreign bodies into the granular body for the calculation; then the interfaces belong to the unknowns of the problem. The natural ground also requires artificial boundaries below and farther away.

Deformations can be markedly delayed in case of insufficient drainage and high viscosity of the grain skeleton. The combination of both effects is briefly outlined here for one-dimensional compression.

Consider a saturated column confined by smooth walls starting from a slurry (Figure 6). The velocities v_s of the grain skeleton and v_f of the water (a) have the same amount and opposite signs because of mass conservation. The filtration law may be written:

$$v_f - v_s = 2v_f = -\frac{k(e)}{\gamma_f}\frac{\partial p_f}{\partial x}, \tag{33}$$

with a permeability k depending on void ratio; let us assume for simplicity's sake:

$$k = k_0 \frac{e}{e_0}, \tag{34}$$

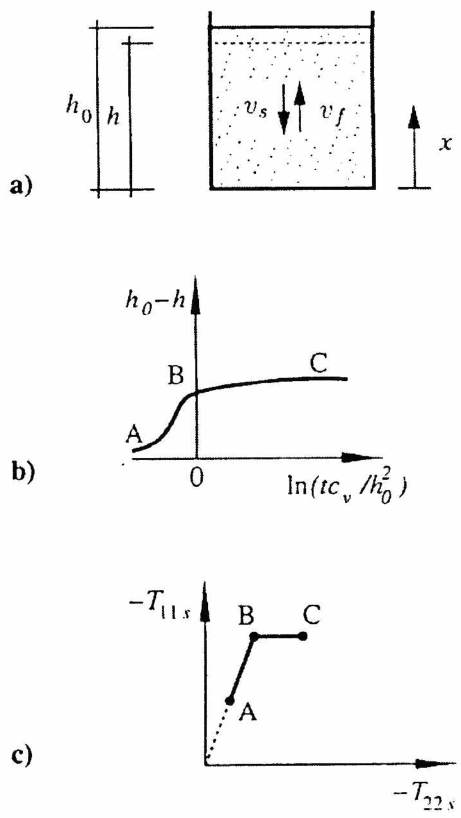

Figure 6. Delayed one-dimensional compression

with $k = k_0$ for $e = e_0$. According to Section 2.4, the compression law can be written as:

$$e = e_0 \exp\left[-\left(\frac{p_s}{h_s}\right)^n\right], \tag{35}$$

with the inter-granular pressure p_s in the direction x. With the total pressure $-T_{11} = -T_{11s} + p_f$ and the balance of momentum (without mass forces), the balance of mass can be combined with Equations (33), (34). With $n = 1$ a rather simple non-linear diffusion equation is obtained for the volumetric fluid fraction $\alpha_f := e/(1+e)$, *viz.*:

$$\frac{\partial \alpha_f}{\partial t} = \frac{1}{2}\frac{h_s k_0}{\gamma_f}\frac{\partial}{\partial x}\left[\frac{1}{(1-\alpha_f)^2}\frac{\partial \alpha_f}{\partial x}\right]. \tag{36}$$

A more complicated equation is obtained for $n > 1$. With the initial condition $\alpha_{f0} = e_0/(1-e_0)$ and the boundary values α_f or $\partial\alpha_f/\partial x$ for $x = 0$ and $x = h$, numerical results can be obtained. They can be plotted conventionally with the aid of $c_v := h_s k_0/\gamma_f$ and look rather familiar for $t < h_0^2/c_v$ (Figure 6b).

The inter-granular stress path is almost straight for this part of the consolidation (path AB in Figure 6b). For times $t >> h_0^2/c_v$ when the gradient of fluid pressure is very low, the vertical granulate pressure T_{11s} remains nearly constant. However, the decrease of h_{sa} with the decrease of $\|\boldsymbol{D}_s\|$ ($D_{11s} = \partial v_s/\partial x$ here) by Equation (28) causes an increase of the lateral pressure T_{22s} (path BC). The further decrease of void ratio is no more described by Equation (36) as the compression is no more proportional. It can be calculated with the aid of Equation (28) by iterative adaption of T_{22s}/T_{11s} and D_{11s}.

For a spherically or cylindrically symmetric compression a diffusion equation similar to Equation (36) is obtained. An allowance for argotropy is rather easy as the condition of isotropy is not left. Numerical solutions are of interest for the evaluation of experiments, *e.g.* shrinkage.

We now turn to the case of creep without drainage of a saturated cylindrical sample (Figure 7a) with a rather high viscosity index. The material may be consolidated from the slurry state to $-T_{22s} = p_0$ and $-T_{11s} = p_0$ (A) or p_0/K_{s0} (B). With an increase of the total stress deviator the rate of axial compression $-D_{11s}$ increases, and keeping it constant then, $-D_{11s}$ decreases with time first and increases later (b). The reduction of sample height with time is smaller for an anisotropic preconsolidation than for the isotropic case, but equal in quality.

This known behaviour (*e.g.* Sekiguchi 1984) can be explained by changes of granulate stresses (Figure 7c) calculated with Equation (5) including $h_{sa} \neq h_s$. The initially isotropic sample undergoes a substantial reduction of pressure p_s, and the pore pressure increases. Under constant $T_{11} - T_{22}$ the reduction of p_s goes on, so that the stress ratio T_{11s}/T_{22s} increases. This requires h_{sa} to increase, *i.e.* $\|\boldsymbol{D}_s\|$ must increase according to Equation (28). The critical state line (c in Figure 7c) is reached. For anisotropic preconsolidation the decrease of p_s is weaker so that the c-line is reached earlier.

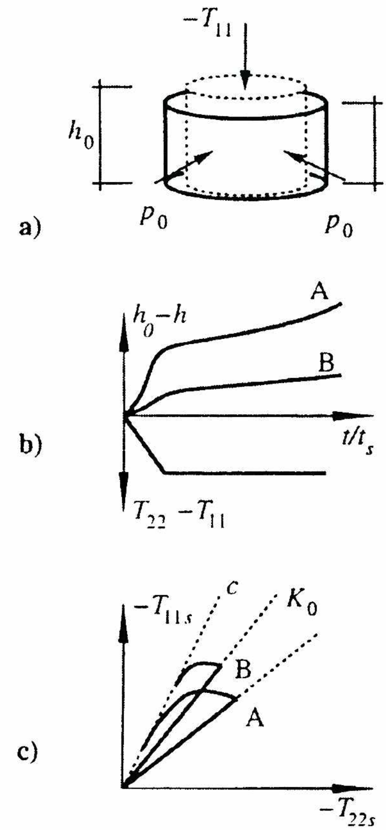

***Figure 7.** Creep without drainage*

An extension to more complicated deformations is rather difficult. A single diffusion equation is no more obtained, and the coupled equations can be mathematically ill-posed. This may lead to a loss of stability (Section 3.3), localisation and/or self-organisation (Section 4.2).

3.3 Stability of equilibrium

An equilibrium state of a granular body may be called unstable if velocity fields $\boldsymbol{v}_s$ can be found which release kinetic energy. With the chinese character for work (in Pinjin gong) this can be written $I(\boldsymbol{v}_s) > 0$. The equilibrium is stable if $I(\boldsymbol{v}_s) < 0$ holds for any $\boldsymbol{v}_s$, and indifferent with respect to a certain $\boldsymbol{v}_s$ if this yields $\mathbf{I} = 0$. The $\boldsymbol{v}_s$-field is called mode of collapse if it leads to $\mathbf{I} > 0$. For indicating the use of our constitutive equation with this kind of stability analysis, we briefly consider samples and slopes with full and without drainage. Argotropy is excluded by taking $h_{sa} = h_s$.

Consider a fully drained cylindrical sample first (Figure 8). The initial state may be $\boldsymbol{T}_s = \mathbf{0}$ and $e = e_{i0}$. The intergranular stress path may be isotropic loading (0A) from the suspension and unloading (AB) afterwards, and loading with constant mean pressure up to the peak then (BP). The void ratio e_A at A can be calculated from

Equation (20), and e_B at B from Equation (5). The equivalent pressure p_{eB} at B, calculated from Equation (27), is slightly lower than p_{eA}. (The ratio of isotropic loading and unloading rates of compression is determined by φ_c via Equations (6) – (8).)

The transition to the peak is calculated with Equation (5) as outlined in Section 2.3. The void ratio increases to a value e_p, and the dilatancy ratio κ, or $-D_{22}/D_{11}$, is maximal at P. The peak stress ratio can be expressed by a friction angle φ_p with Equation (18), or by the equivalent angle φ_p in Figure 8. The peak dilatancy and friction ratios increase with the ratio of equivalent and mean inter-granular pressure, $-p_e/p_s$. The locus L of peak stresses is curved therefore and leads to 0. A section of it may be approximated by a Coulomb envelope C with a pressure independent 'effective friction angle' φ', and an 'effective cohesion' c' proportional to p_e. This behaviour was proposed by Hvorslev (1960) and is incorporated in the original Cam Clay theory (Schoefield and Wroth 1968).

Such calculations can be made for other homogeneous deformations as cylindrical extension, biaxial and simple shearing. The curves are similar, but the parameters κ_p, φ_p, φ' and c'/p_e are not the same. This dilemma is overcome by means of a stability analysis with a linearly distributed velocity field $\boldsymbol{v}_s$ (as required for element tests). The state variables e and $\boldsymbol{T}_s$, which may result from any history, can lead to $\mathbf{I} > 0$ with:

$$\mathbf{I} := -\mathrm{tr}\,(\overset{\backslash}{\boldsymbol{T}}_s \nabla \boldsymbol{v}_s)V, \tag{37}$$

if the boundary stresses are dead loads (Hill 1958). The symbol $\mathbf{I}$ is used as this quantity is different from conventional energies. V is the sample volume, and $\overset{\backslash}{\boldsymbol{T}}_s$ is a nominal stress rate defined by:

$$\overset{\backslash}{\boldsymbol{T}}_s = \overset{\circ}{\boldsymbol{T}}_s + \boldsymbol{W}_s\boldsymbol{T}_s - \boldsymbol{T}_s\boldsymbol{W}_s + \boldsymbol{T}_s\,\mathrm{tr}\,\boldsymbol{D}_s\,. \tag{38}$$

As $\overset{\circ}{\boldsymbol{T}}_s$ is homogeneous of the first order with respect to $\boldsymbol{D}_s$ by Equation (5), $\mathbf{I}$ is homogeneous of the second order in $\boldsymbol{v}_s$ (as the kinetic energy). A positive scalar factor in $\boldsymbol{v}_s$ has no influence on the sign of $\mathbf{I}$.

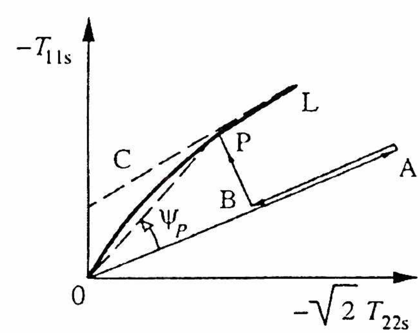

Figure 8. *Drained cylindrical compression up to peak*

The variation of $\boldsymbol{v}_s$ is restricted by the dilatancy ratio from Equation (11). States with $\mathbf{I} = 0$, which may be called limit equilibrium states, can thus be found. They do not coincide with peak states, but can be close to them. Strength parameters are not needed for this stability analysis, but they can be helpful in special cases.

Undrained element tests with saturated granular material can be analyzed likewise with $\mathbf{I}$. The fluid pressure p_f enters as an additional state variable via Equation (1), and $\operatorname{tr}\boldsymbol{D}_s = 0$ holds for incompressible grains and fluid. A strength parameter c_u ('undrained cohesion') can be calculated for different stress ratios $\hat{\boldsymbol{T}}_s$ and stretching directions $\vec{\boldsymbol{D}}_s$ but it is not needed.

The transfer to inhomogeneous fields may be indicated for a submerged slope with saturated granular material (Figure 9). The field of state variables e, $\boldsymbol{T}_s$ and p_f has to be estimated from field data, boundary conditions and balance equations. This field cannot uniquely be determined, but measured data and strength parameters help to restrict its range. Modes of collapse $\boldsymbol{v}_s$, with $\operatorname{tr}(\nabla \boldsymbol{v}_s) = 0$ in this case, have to be assumed from experience (dashed in Figure 9). The stability can be judged from the sign of:

$$\mathbf{I} := -\int \operatorname{tr}\left(\overset{\wedge}{\boldsymbol{T}}_s \nabla \boldsymbol{v}_s\right) \mathrm{d}V. \tag{39}$$

Simplified $\boldsymbol{v}_s$-fields suffice because of the uncertainty of state and the averaging property of the integral (Gudehus 1993). This method has been verified for fine sands (Raju 1994).

The extension to more complicated systems is principally straightforward. $\mathbf{I}$ (which can be looked upon as a kind of Liapunov function) has to be modified if not only dead loads occur. Modes of collapse $\boldsymbol{v}_s$ can also be obtained numerically by systematic variation of imperfections (Tejchman 1994). Due to the non-linearity of Equation (5) they are no eigenvectors, and $\mathbf{I}$ is not a potential. Shear localisations can be incorporated (Section 4.2). The modes have to be varied in order to find the one which first yields $\mathbf{I} > 0$. An allowance for viscous and inertial effects will be more difficult (Section 4.2).

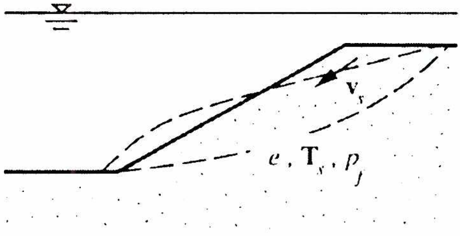

Figure 9. *Slope collapse with undrained saturated material*

3.4 Granular flow

Our constitutive equation can also be used for the analysis of granular flow. Penetration is included as it can be looked upon as granular flow around a fixed obstacle. It is briefly shown how Equation (5) can be used for stationary flow of undrained and fully drained granular bodies. Some remarks on stability are added.

Undrained stationary flow of saturated bodies is kinematically the simplest case because of $\mathrm{tr}(\nabla \boldsymbol{v}_s) = 0$. Stationarity requires $\partial(\cdot)/\partial t \equiv 0$ for the state variables e, $\boldsymbol{T}_s$, p_f and the velocity field $\boldsymbol{v}_s$. A non-linear set of differential equations for these quantities results from the balance equations and Equations (1), (5). Viscosity can be incorporated with Equation (28). Boundary conditions have to be written for $\boldsymbol{T}_s$, p_f and $\boldsymbol{v}_s$. An iterative algorithm with stepwise improvement of stretching direction $\vec{\boldsymbol{D}}_s$ is required (*cf.* Winter 1979). It is not necessary and not even helpful to assume a constant "undrained cohesion". e is part of the solution in general and can deviate from e_c.

Solutions may be found, but they can be unstable. Imagine an inclined open channel with a granular mass flowing due to gravity, *e.g.* a creeping clay slope (Figure 10). The stationary solution, with a velocity profile $\boldsymbol{v}_{s1}$, may be given. (Without inertial effects it may be called a flow equilibrium.) A wavy mode $\boldsymbol{v}_{s2}$ may

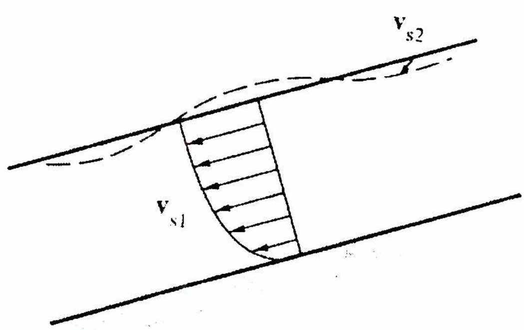

Figure 10. *Instability of a creeping slope*

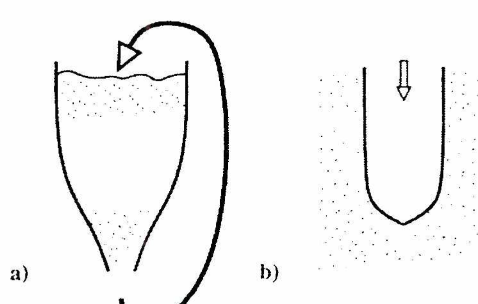

Figure 11. *Examples of drained stationary flow*

arise so that the flow becomes pulsating. Without inertial effects $\boldsymbol{v}_{s2}$ can be detected with Equation (39) by $\mathbf{I} > 0$. A similar result can be obtained for stretching of a strip: the symmetry-breaking waves may then be called necking.

For drained stationary flow changes of density occur, *i.e.* $\mathrm{tr}(\nabla \boldsymbol{v}_s) \neq 0$ in general. Consider two examples without pore fluid (Figure 11). The granular material flowing through a convergent channel (a) has to be refilled in order to keep the surface in place. The penetration of a wall or rod (b) can cause a stationary flow of the surrounding granular body if this is initially homogeneous in the axial direction. The fields e, $\boldsymbol{T}_s$, $\boldsymbol{v}_s$ may be calculated from boundary conditions, the conservation laws and Equation (5). These states are not critical everywhere, *i.e.* $e \neq e_c$, and $\boldsymbol{T}_s \neq \boldsymbol{T}_{sc}$ hold in general.

Again, such solutions can be unstable. Shear localisations may occur, and the flow may become pulsating or chaotic. An analysis is possible with an extension of our constitutive equation (Tejchman 1994). No criterion for such dynamic instability has yet been found.

4. Limitations and extensions

4.1 Choice of functions

Leaving aside the basic assumption implied by Equation (4), the choice of functional representations is not free from arbitrariness. We first discuss the choice of the functions in Equation (5), and then the concept of factorial decomposition. When evaluating special experimental results one is inclined to improve one or the other of the chosen functions. However, it is not advisable to modify them only for a better adaption to a few tests.

Other representations for $\boldsymbol{L}$ and $\boldsymbol{N}$ satisfying the requirements of Section 2.1 can be found (Bauer 1996). The stress ratio tensor may be replaced by the direction tensor $\vec{\boldsymbol{T}}_s := \boldsymbol{T}_s / \|\boldsymbol{T}_s\|$. Other representations for f_e and f_d, depending only on the ratios e/e_c and e_d/e_c, in order to avoid pressure dependence, can be given within the desired limits. The choice of Equation (20), and therefore f_b via Equation (26), will also not be once and for ever. Improvements may be justified by further element tests. Apart from experimental problems with coarse hard grains (bedding errors), the influence of honeycombs and clods should, however, first be clarified (Section 4.2).

One can introduce other representations for h_{sa} instead of Equation (28), leading likewise to the behaviour outlined in Figures 5-7. Argotropy can also be modelled by transferring Perzyna's concept of overstress from elasto-plasticity to hypoplasticity (Wu *et al.* 1993). This leads to additional state variables, however (Section 4.2).

The non-linear term of Equation (5) vanishes for $f_d \to 0$, so that the material becomes hypoelastic. This appears plausible: for maximal density the hysteretic damping can be very low. Resonant column tests with cohesionless materials indicate that, with decreasing amplitudes of cyclic shearing, the shear modulus is almost independent of strain amplitude, and damping disappears. A perfect shakedown of this kind is not possible with Equation (5), except for $e = e_d$ so that the non-linear part disappears. Granular materials with $e \approx e_c$ do not show a shakedown: they are densified or liquified even with small strain amplitudes. Materials with a medium void ratio do not show a perfect shakedown, but their behaviour is rather hypoelastic for very low stretching amplitudes.

It would be desirable to reformulate the constitutive equation so that linearity can be obtained for $e > e_d$. This cannot be achieved, however, by any function of $\boldsymbol{T}_s$ and $\boldsymbol{D}_s$ only. In order to unify hypoplasticity, pyknotropy and argotropy one can think of introducing an intrinsic stress tensor as additional (internal) variable, as was proposed by Kolymbas (1988). The physical reason for an internal stress can be the absorbed part of the pore fluid. The state of absorbed pore fluid can be changed by deformations.

Añ extension to partly saturated materials is rather straightforward with the aid of capillarity and will be treated in a later publication. Barotropy of the proposed kind has a serious shortcoming: the destruction of grains is not covered and can lead to problems for the case of a substantial reduction of pressure after a strong compression. One could correct the set of parameters for the change of grain size. Our constitutive equation is therefore restricted to $p_s < ca10^{-2}\ h_s$.

4.2 Choice of variables

Equation (5) implies the assumption that the state is sufficiently characterised by a symmetric inter-granular stress tensor and by the void ratio only. As outlined in Section 4.1, it appears that an intrinsic stress tensor is required to overcome this principal restriction. More properly, the bonded pore fluid should be treated as an additional constituent. More complicated states are also connected with localisations, clods and honeycombs, and cracks.

Localisations are zones of dilation with a thickness proportional to the mean grain diameter (Gudehus 1994). They can develop along interfaces with foreign bodies and inside granular bodies. Bodies with dilatancy under dead loads tend to a single localisation and subsequent collapse, whereas kinematic constraints can lead to regular localisation patterns. Any mechanical model must then imply a material length, preferably the mean grain size. A corresponding extension of the present constitutive equation has been achieved (Tejchman 1994)

Granular structures with clods or honeycombs are possible with suitable bonding forces. They can be destroyed, but not reconstituted by uniform deformations. Granulates with void ratios exceeding e_c (*cf.* Section 2.4) are prone to collapse. The description of state by stress tensor and void ratio is insufficient then: one has to introduce additional tensorial variables both for the pore system and the internal forces. This range of pressures is avoided by $p_s < ca10^{-6}\ h_s$.

Cracks are likewise not covered by our concept of state. The void ratio of a crystalline rock body cracked into blocks can be well below e_d defined in Section 2.3. One can analyse a localised fracture with the aid of some internal length (with a surface energy contribution to **I**). Higher order kinematic and static state variables are required then. For these reasons the proposed theory cannot explain certain mechanisms of tectonics and of ploughing. Theories of self-organisation in granular bodies have still to be developed for such cases.

Acknowledgement

This treatise is based on more than 25 years of research work in Karlsruhe. Main contributions are due to Prof. D. Kolymbas, who has also supported this paper by valuable criticisms. Among the more recent contributions, those by Dr. E. Bauer are most important; he reports on his work in the companion paper. Among the users of hypoplastic equations, H. Hügel has especially contributed by numerical tests. Valuable hints from Dr. A. Niemunis and Dr. P. v. Wolffersdorff are also gratefully acknowledged.

References

[1] Bauer E. and Wu W., *A hypoplastic model for granular soils under cyclic loading*, Proc. Int. Workshop on Modern Approaches to Plasticity for Granular Materials, Horton, Greece, Kolymbas D. (ed), Elsevier, 1993

[2] Bauer E., *Calibration of a comprehensive hypoplastic model for granular materials*, Soils and Foundations, Jap. Soc. Soil Mech. **36**, 13, 1996

[3] De Boer P. and Ehlers W., *Upon friction and capillarity*, Int. Journ. Solids Structures, **26**, 43, 1990

[4] Gudehus G., *A comparison of some constitutive laws for soils under radially symmetric loading and unloading*, Proc. Conf. on Num. Meth. in Geomech., Aachen 1309, 1979

[5] Gudehus G., *Bodenmechanik*, Enke, Stuttgart, 1981

[6] Gudehus G., *Seitendruck auf pfählen in tonigen Böden*, Geotechnik **2/84**, 73, 1984

[7] Gudehus G., *Spontaneous liquefaction of saturated granular bodies*, Proc. Int. Workshop Modern Approaches to Plasticity for Granular Materials, Horton, Greece, Kolymbas D. (ed.), Elsevier, 1993

[8] Gudehus G., *Localization in granular bodies – position and objectives*, Localization and Bifurcation Theory for Soils and Rocks, Chambon R. *et al.* (eds.), Balkema 3, 1994

[9] Hill R., *A general theory of uniqueness and stability in elastic-plastic solids*, Jour. of the Mech. and Phys. of Solids **6**, 236, 1958

[10] Hvorslev M. J., *Physical components of the shear strength of saturated clays*, in: Shear Strength of Cohesive Soils, ASCE, Univ. of Colorado 169, 1960

[11] Kolymbas D., *Eine konstitutive Theorie für Böden und andere granulare Stoffe*, Veröffentlichungen des Instituts für Bodenmechanik und Felsmechanik der Universität Karlsruhe, Heft 109, 1988

[12] Kolymbas D., *An outline of hypoplasticity*, Arch. App. Mech. **61**, 143, 1991

[13] Kolymbas D. and Wu W., *Introduction to hypoplasticity*, Proc. Int. Workshop on Modern Approaches to Plasticity for Granular Materials, Horton, Greece, Kolymbas D. (ed.), Elsevier, 1993

[14] Leinenkugel H. J., *Deformations und Festigkeitsverhalten Bindiger Erdstoffe – Experimentelle Ergebnisse und Physikalische Deutung*, Veröffentlichungen des Instituts für Bodenmechanik und Felsmechanik der Universität Karlsruhe, Heft 67, 1976

[15] Raju V. R., *Spontane Verflüssigung lockerer granularer Korper-Phanomene, Ursachen, Vermeidung*, Veröffentlichungen des Instituts für Bodenmechanik und Felsmechanik der Universität Karlsruhe, Heft 132, 1994

[16] Schoefield A. and Wroth R., *Critical State Soil Mechanics*, Mc Graw Hill, London, 1968

[17] Sekiguchi H., *Theory of undrained creep rapture of normally consolidated clay based on elasto-viscoplasticity*, Soils and Foundations **24**, 129, 1984

[18] Tejchman J., *Numerical study on localized deformation in a Cosserat continuum*, Localization and Bifurcation Theory for Soils and Rocks, Chambon R. *et al.* (eds.), Balkema 257, 1994

[19] Winter H., *Fließen von Tonböden: Eine mathematische Theorie und ihre Anwendung auf den Fließwiderstand von Pfählen*, Veröffentlichungen des Instituts für Bodenmechanik und Felsmechanik der Universität Karlsruhe, Heft 82, 1979

[20] Wu W. and Bauer E., *A hypoplastic model for barotropy and pyknotropy of granular soils*, Proc. Int. Workshop on Modern Approaches to Plasticity for Granular Materials, Horton, Greece, Kolymbas D. (ed.), Elsevier, 1993

[21] Wu W., Bauer E., Niemunis A. and Herle I., *Viscohypoplastic models for cohesive soils*, Proc. Int. Workshop on Modern Approaches to Plasticity for Granular Materials, Horton, Greece, Kolymbas D. (ed.), Elsevier, 1993